Nonlinear gyrokinetic theory and its application to computation of the gyrocenter motion in ripple field

Siqiang Zhu' , Yingfeng Xu, and Shaojie Wang

Citation: Physics of Plasmas **23**, 062306 (2016); doi: 10.1063/1.4953544
View online: http://dx.doi.org/10.1063/1.4953544
View Table of Contents: http://aip.scitation.org/toc/php/23/6
Published by the American Institute of Physics

Nonlinear gyrokinetic theory and its application to computation of the gyrocenter motion in ripple field

Siqiang Zhu,[1,a)] Yingfeng Xu,[2] and Shaojie Wang[1]
[1]*Department of Modern Physics, University of Science and Technology of China, Hefei 230026, China*
[2]*Institute of Plasma Physics, Chinese Academy of Science, Hefei, Anhui 230031, China*

(Received 28 January 2016; accepted 26 May 2016; published online 14 June 2016)

The nonlinear gyrokinetic equation with full electromagnetic potential perturbations is derived by using the two-step transform procedure. The second-order transformed Hamiltonian can be simplified as $\frac{1}{2}\delta A_{\parallel}^2$, instead of $\frac{1}{2}\delta \boldsymbol{A}^2$ in the long-wave-length limit. A numerical code based on the I-transform method is improved to compute the gyrocenter orbit in the TFTR tokamak with a ripple field, and the numerical results indicate that the collisionless stochastic diffusion criterion agrees well with the theoretical prediction. *Published by AIP Publishing.*
[http://dx.doi.org/10.1063/1.4953544]

I. INTRODUCTION

The turbulence transport is a very important topic in the tokamak transport research. The micro-instabilities related to turbulence are often investigated by using the nonlinear gyrokinetic (GK) theory[1–8] and numerical GK simulations.[9–17] In the modern gyrokinetic theory,[4–8,18–24] the Lie-transform perturbation method[25–28] is used to decouple the gyrocenter (GY) motion from the gyromotion. Then, the kinetic equation can be reduced to the gyrokinetic equation, which is much easier to investigate the evolution of the tokamak plasma on the timescale longer than the gyro-period.

The Lie-transform is a very powerful systematic method to treat the perturbation problem. The GK equations based on the two-step transform developed by Hahm *et al.*[6] have been widely used in the electromagnetic GK simulation.[16,17,24] In Hahm's transform procedure, the $\delta A_{\parallel}$ term is moved into the Hamiltonian part firstly, which makes all the perturbations appear in the Hamiltonian part and keep the transformed Poisson bracket formally same as the unperturbed (UP) one; then, the conventional transform, in which the gauge function S_n is used to remove the gyroangle-dependent part of the physical quantities, is used to derive the nonlinear GK equation. And, the two-step transform has been applied to full electromagnetic potential perturbation in arbitrary field geometry to study the transport of the GK turbulence.[20,24]

Recently, the I-transform method has been developed to decouple the perturbation part of the motion from the unperturbed motion, which is useful in the kinetic and GK theory.[19–21] The I-transform method has been used to make the transport analysis in the one-dimensional Vlasov-Poisson system.[29] The code NLT based on the I-transform method is developed to compute the guiding-center (GC) orbit of particles in magnetic islands in a tokamak,[24] and the results agree with the code GYCAVA,[22] which is based on the conventional Lie-transform perturbation method. However, the perpendicular component of the magnetic potential perturbation is not fully contained in the NLT code, which is related to the second-order transformed Hamiltonian.

Considering the particle motion in the ripple field, which is generated by the discreteness of toroidal field coils, one has to deal with the perpendicular magnetic vector potential perturbation. The well confinement of the fusion product alpha particles is an important condition to achieve ignition in tokamak fusion reactors. The ripple field causes enhancement of the loss of the alpha particles, devoting locally strong heat loads on the wall. Goldston, White, and Boozer (GWB) theoretically predicted a critical value of ripple field for collisionless stochastic diffusion in the thin banana approximation,[30] which has been verified by Tani by using an orbit-following Monte-Carlo code.[31] Simulation results are generally consistent with the GWB model.[32–34] And, the stochastic ripple diffusion was observed experimentally by Boivin in TFTR.[35]

In this paper, the second-order transformed Hamiltonian is investigated in detail. The result shows that the main term of the second-order transformed Hamiltonian is $\frac{1}{2}\delta A_{\parallel}^2$ for any magnetic perturbation in the long-wave-length limit. The NLT code is improved based on the theory above to compute the GC orbit of particles in TFTR with a ripple field. The results are consistent with those computed by the code GYCAVA.

The remaining part of this paper is organized as follows. In Sec. II, we present the fundamental equations about Hamiltonian theory of the gyrocenter motion; in Sec. III, the GK equation based on the two-step transform procedure and the I-transform method is derived; in Sec. IV, the improved NLT code is used to compute the GC orbit in TFTR with the ripple field; in Sec. V, the main results are summarized.

II. REVIEW OF THE FUNDAMENTALS

A. Hamiltonian theory of the unperturbed guiding-center motion

We begin with the Hamiltonian theory of the GC motion in the unperturbed (UP) electromagnetic field.[36–38] The UP fundamental one-form (the GC Lagrangian) is written in

[a)]E-mail: zhusq@mail.ustc.edu.cn

terms of the noncanonical variables $Z^i = (\boldsymbol{X}, v_\parallel, \mu, \xi)$ as $\hat{\Gamma}_0 \equiv \Gamma_0 - H_0 dt$; the UP symplectic part and the UP Hamiltonian are

$$\Gamma_0 \equiv \Gamma_{0i} dZ^i = (v_\parallel \boldsymbol{b}_0(\boldsymbol{X}) + \boldsymbol{A}_0(\boldsymbol{X})) \cdot d\boldsymbol{X} + \mu d\xi, \tag{1a}$$

$$H_0(\boldsymbol{X}, v_\parallel, \mu) = \frac{1}{2} v_\parallel^2 + \mu B_0, \tag{1b}$$

where $\boldsymbol{X}$ is the GC position, $v_\parallel$ is the parallel velocity, μ is the magnetic moment, ξ is the gyroangle, respectively; $\boldsymbol{b}_0 = \boldsymbol{B}_0/B_0$, with $\boldsymbol{B}_0 = \nabla \times \boldsymbol{A}_0$ as the UP magnetic field. The problem with equilibrium scalar field ϕ_0 has been discussed in Refs. 38–40. In this paper, we set the electrical charge and mass of particle to be unity for simplicity, and it is easy to restore the physical formulae by checking the units of the physical variables. The GC motion is determined by the symplectic structure and the Hamiltonian.

The Lagrange two-form is defined as $\omega \equiv d\Gamma$. The UP Lagrange two-form is written as $\hat{\omega}_0 \equiv \omega_0 - dH_0 \wedge dt$, and

$$\omega_0 = \frac{1}{2} \epsilon_{ijk} B_0^{*k} dX^i \wedge dX^j + b_{0j} dv_\parallel \wedge dX^j + d\mu \wedge d\xi, \tag{2}$$

with $\boldsymbol{B}_0^* = \boldsymbol{B}_0 + v_\parallel \nabla \times \boldsymbol{b}_0$, d as the exterior differential, $\wedge$ as the exterior product, ϵ_{ijk} as the permutation tensor, and b_{0j} as the component of $\boldsymbol{b}_0$.

The UP equations of GC motion are

$$\dot{Z}_0^i = \{Z^i, H_0\} = \{Z^i, Z^j\} \partial_j H_0 \equiv J_0^{ij} \partial_j H_0, \tag{3}$$

where J_0^{ij} is the component of the UP Poisson matrix J_0 which is simply the inverse matrix of ω_0. And, the non-zero components of J_0 are $J_0^{X^i X^j} = -\frac{\epsilon^{ijk} b_{0k}}{B_{\parallel 0}^*}$, $J_0^{X^i v_\parallel} = -J_0^{v_\parallel X^i} = \frac{B_0^{*i}}{B_{\parallel 0}^*}$, $J_0^{\xi\mu} = -J_0^{\mu\xi} = 1$, with $B_\parallel^*(\boldsymbol{X}, v_\parallel) = \boldsymbol{B}_0^* \cdot \boldsymbol{b}_0$ is the Jacobian of the GC phase space coordinate $(\boldsymbol{X}, v_\parallel, \mu, \xi)$. The UP GC Vlasov equation is

$$\partial_t F_0 + \{F_0, H_0\} = 0. \tag{4}$$

And, its solution, the GC distribution function $F_0(\boldsymbol{X}, v_\parallel, \mu)$, is a constant of motion.[18,41–43]

B. Lie-transform Hamiltonian perturbation method

In a perturbed Hamiltonian system with a parameter ϵ_δ, which denotes the ratio of the perturbations respect to the equilibrium quantities, the fundamental one-form $\hat{\Gamma} \equiv \Gamma - H dt$ can be expanded in powers of the small parameter ϵ_δ

$$\hat{\Gamma} = \hat{\Gamma}_0 + \hat{\Gamma}_1 + \hat{\Gamma}_2 + \cdots, \tag{5a}$$

$$\Gamma = \Gamma_0(\boldsymbol{Z}) + \Gamma_1(\boldsymbol{Z}, t) + \Gamma_2(\boldsymbol{Z}, t) + \cdots, \tag{5b}$$

$$H = H_0(\boldsymbol{Z}) + H_1(\boldsymbol{Z}, t) + H_2(\boldsymbol{Z}, t) + \cdots, \tag{5c}$$

with $H_1/H_0 \sim \epsilon_\delta$, $H_2/H_0 \sim \epsilon_\delta^2$. Lie-transform is a method to simplify the equations of motion by transforming the coordinates $\boldsymbol{Z}$ to another coordinates $\bar{\boldsymbol{Z}}$. In the coordinates $\bar{\boldsymbol{Z}}$, the fundamental one-form $\bar{\hat{\Gamma}} \equiv \bar{\Gamma} - \bar{H} dt$, same as $\hat{\Gamma}, \Gamma, H$, can be expanded in powers of ϵ_δ. We use T to denote the transform from $\boldsymbol{Z}$ to $\bar{\boldsymbol{Z}}$; the transformation between coordinates, scalar functions, and the fundamental one-form are $\bar{Z} = TZ$, $\bar{F} = T^{-1}F$, $\bar{\hat{\Gamma}} = T^{-1}\hat{\Gamma} + dS$. Up to $\mathcal{O}(\epsilon_\delta^2)$, the relations of the coordinates are written as

$$\bar{Z}^i = Z^i + G_1^i(Z) + G_2^i(Z) + \frac{1}{2} G_1^j \partial_j G_1^i(Z), \tag{6a}$$

$$Z^i = \bar{Z}^i - G_1^i(\bar{Z}) - G_2^i(\bar{Z}) + \frac{1}{2} G_1^j \partial_j G_1^i(\bar{Z}), \tag{6b}$$

and the transform relations between functions F and $\bar{F}$ are

$$F = \bar{F} + G_1^i \partial_i \bar{F} + G_2^i \partial_i \bar{F} + \frac{1}{2} G_1^j \partial_j (G_1^i \partial_i \bar{F}), \tag{7a}$$

$$\bar{F} = F - G_1^i \partial_i F - G_2^i \partial_i F + \frac{1}{2} G_1^j \partial_j (G_1^i \partial_i F), \tag{7b}$$

which indicates the scalar invariance, $F(\boldsymbol{Z}) = \bar{F}(\bar{\boldsymbol{Z}})$. The relation of the fundamental one-form is[5,26]

$$\bar{\hat{\Gamma}}_0 = \hat{\Gamma}_0, \tag{8a}$$

$$\bar{\hat{\Gamma}}_1 = \hat{\Gamma}_1 - L_1 \hat{\Gamma}_0 + dS_1, \tag{8b}$$

$$\bar{\hat{\Gamma}}_2 = \hat{\Gamma}_2 - L_1 \hat{\Gamma}_1 + \left(\frac{1}{2} L_1^2 - L_2 \right) \hat{\Gamma}_0 + dS_2, \tag{8c}$$

where L_ns are the Lie derivatives generated by the generating vector field $\boldsymbol{G}_n$, $L_n = \boldsymbol{G}_n \cdot d$ and S_ns are the gauge functions. Eq. (8) can be explicitly written as

$$\bar{\Gamma}_{1j} = \Gamma_{1j} - G_1^i \omega_{0ij} + \partial_j S_1, \tag{9a}$$

$$\bar{H}_1 = H_1 - \boldsymbol{G}_1 \cdot d H_0 - \partial_t S_1, \tag{9b}$$

$$\bar{\Gamma}_{2i} = \Gamma_{2i} - \frac{1}{2} G_1^k (\omega_{1kj} + \bar{\omega}_{1kj}) - G_2^i \omega_{0ij} + \partial_j S_2, \tag{9c}$$

$$\bar{H}_2 = H_2 - \boldsymbol{G}_1 \cdot d H_1 + \frac{1}{2} \boldsymbol{G}_1 \cdot d(\boldsymbol{G}_1 \cdot d H_0) - \boldsymbol{G}_2 \cdot d H_0 - \partial_t S_2 - \frac{1}{2} G_1^i \partial_t (\Gamma_{1i} + \bar{\Gamma}_{1i} - \partial_i S_1). \tag{9d}$$

We can simplify $\bar{\hat{\Gamma}}$ by choosing an appropriate form of $\boldsymbol{G}_n, S_n$. Making the symplectic part of the transformed fundamental one-form same as the UP one, we have

$$\bar{\Gamma}_{0i} = \Gamma_{0i}, \tag{10a}$$

$$\bar{\Gamma}_{1i} = 0, \tag{10b}$$

$$\bar{\Gamma}_{2i} = 0, \tag{10c}$$

$$\bar{H}_0 = H_0, \tag{10d}$$

$$\bar{H}_1 = \delta\Psi_1 - \{S_1, H_0\} - \partial_t S_1, \tag{10e}$$

$$\bar{H}_2 = \delta\Psi_2 - \{S_2, H_0\} - \partial_t S_2, \tag{10f}$$

$$\delta\Psi_1 = H_1 - \Gamma_{1j} J_0^{ji} \partial_i H_0, \tag{10g}$$

$$\delta\Psi_2 = H_2 - \left(\Gamma_{2j} - \frac{1}{2} G_1^k \omega_{1kj} \right) J_0^{ji} \partial_i H_0 - \frac{1}{2} G_1^i [\partial_i (H_1 + \bar{H}_1) + \partial_t \Gamma_{1i}], \tag{10h}$$

$$G_1^i = (\Gamma_{1j} + \partial_j S_1) J_0^{ji}, \tag{10i}$$

$$G_2^i = \left(\Gamma_{2j} - \frac{1}{2} G_1^k \omega_{1kj} + \partial_j S_2\right) J_0^{ji}. \tag{10j}$$

The flexibility of the Lie-transform method is that the free choices of the form of the gauge functions S_n, which means that we can simplify the analysis by choosing an appropriate form of S_n. For example, S_ns are chosen to remove the gyroangle-dependent part of the transformed Hamiltonian in the usual GK Lie-transform, and in the I-transform, S_ns are used to transform the perturbed Hamiltonian away so that the transformed equations of motion have the same form as the unperturbed ones. The two transforms will be used in Sec. III.

III. NONLINEAR GYROKINETIC EQUATIONS OF MOTION

In this section, three kinds of transform: the $\delta \boldsymbol{A}$ transform, the gyrocenter transform, and the I-transform are presented. The first two transform is used to derive the nonlinear equations of gyro-center (GY) (guiding center in perturbed fields) motion, and I-transform is used to solve the GY equations.

A. The δA transform

In the nonlinear GK theory, the amplitude of the perturbations is much smaller than the corresponding equilibrium quantities, that is, $\frac{|\delta \boldsymbol{E}|}{v_{th} B_0} \sim \frac{|\delta \boldsymbol{B}|}{B_0} \sim \frac{\delta F}{F_0} \sim \epsilon_0 \ll 1$; here, $(\delta \boldsymbol{E}, \delta \boldsymbol{B})$ are the perturbed electromagnetic fields defined as $\delta \boldsymbol{B} = \nabla \times \delta \boldsymbol{A}, \delta \boldsymbol{E} = -\partial_t \delta \boldsymbol{A} - \nabla \delta \phi$, v_{th} is the thermal velocity of the particles, δF and F_0 are the perturbation part and UP part of the distribution function, respectively. The fundamental one-form is $\hat{\Gamma} = \hat{\Gamma}_0 + \hat{\Gamma}_1, \hat{\Gamma}_1 = \Gamma_1 - H_1 dt$

$$\Gamma_1 = \delta \boldsymbol{A}(\boldsymbol{X} + \boldsymbol{\rho}_0, t) \cdot d(\boldsymbol{X} + \boldsymbol{\rho}_0), \tag{11a}$$

$$H_1 = \delta \phi(\boldsymbol{X} + \boldsymbol{\rho}_0, t). \tag{11b}$$

The first order Lagrange two-form $\hat{\omega}_1$ is given by

$$\hat{\omega}_1 = d\hat{\Gamma}_1 = \frac{1}{2} \omega_{1ij} dZ^i \wedge dZ^j - (\partial_t \Gamma_{1i} + \partial_i H_0) dZ^i \wedge dt, \tag{12a}$$

$$\omega_{1ij} = \partial_i \Gamma_{1j} - \partial_j \Gamma_{1i}. \tag{12b}$$

First, the perturbation part of the magnetic potential $\delta \boldsymbol{A}$ shall be transformed into the Hamiltonian part by using the δA transform. We use T_A to represent the transform from GC coordinates $\boldsymbol{Z}$ to a new coordinates $\boldsymbol{Z_A}$ and set the gauge functions $S_n = 0$; then, according to Eq. (9), we can obtain the generating vector field $\boldsymbol{G}_A$

$$G_{A1}^i = \delta \boldsymbol{A} \cdot \partial_j (\boldsymbol{X} + \boldsymbol{\rho}_0) J_0^{ji}, \tag{13a}$$

$$G_{An}^i = 0, (n \geq 2), \tag{13b}$$

where the identity condition[38] $\{\boldsymbol{X} + \boldsymbol{\rho}_0, \boldsymbol{X} + \boldsymbol{\rho}_0\} = 0$ is used, that is

$$\partial_\xi \rho_0^i \partial_\mu \rho_0^j - \partial_\xi \rho_0^j \partial_\mu \rho_0^i = \frac{\epsilon_{ijk} b_{0k}}{B_{\|0}^*}. \tag{14}$$

Eq. (13b) shows that the $\delta \boldsymbol{A}$ transform is an exact transform.[20] The components of generating field $\boldsymbol{G}_A$ can be explicitly written as

$$G_{A1}^{\boldsymbol{X}} = -\frac{\boldsymbol{b}_0}{B_{\|0}^*} \times \delta \boldsymbol{A}, \tag{15a}$$

$$G_{A1}^{v_\|} = \frac{\boldsymbol{B}_0^*}{B_{\|0}^*} \cdot \delta \boldsymbol{A}, \tag{15b}$$

$$G_{A1}^{\xi} = -\delta \boldsymbol{A} \cdot \partial_\mu \boldsymbol{\rho}_0, \tag{15c}$$

$$G_{A1}^{\mu} = \delta \boldsymbol{A} \cdot \partial_\xi \boldsymbol{\rho}_0. \tag{15d}$$

According to Eqs. (14) and (15), we can show that

$$G_{A1}^i \partial_t \Gamma_{1i} = 0, \tag{16}$$

then we can obtain the transformed Hamiltonian from Eq. (10)

$$\begin{aligned} H_{A1} &= H_1 - \boldsymbol{G}_{A1} \cdot dH_0 \\ &= \delta \phi - \delta \boldsymbol{A} \cdot (\dot{\boldsymbol{X}} + \dot{\boldsymbol{\rho}_0}), \end{aligned} \tag{17}$$

$$\begin{aligned} H_{A2} &= \frac{1}{2} \boldsymbol{G}_{A1} \cdot d(\boldsymbol{G}_{A1} \cdot dH_0) \\ &= \frac{1}{2} \delta \boldsymbol{A}^2, \end{aligned} \tag{18}$$

which clearly indicates the scalar invariance. Note that all the perturbations have been transformed into the Hamiltonian part; the symplectic part of the transformed fundamental one-form is kept formally same as the unperturbed one, which is the effect of the $\delta \boldsymbol{A}$ transform. The results are the same as those of previous,[24] and it would recover Hahm's results if only considering the parallel perturbation $\delta A_\|$.[6] Note that it has been shown that we can obtain the same results intuitively from the physical view of transforming the particle coordinates.[20]

B. The gyrocenter transform

The gyrocenter transform shall be used to search a new coordinate, called gyrocenter coordinates, in which the gyrocenter motion is decoupled from gyromotion and the new magnetic moment is a constant of motion. For this purpose, we should choose an appropriate gauge functions S_n to remove the gyroangle-dependent part. T_Y denotes the transform from the coordinates $\boldsymbol{Z_A}$ to the GY coordinates $\bar{\boldsymbol{Z}}, \bar{Z}^i = T_Y Z_A^i$. According to Eq. (10), up to second order, we get the generating vector $\boldsymbol{G}_{Yn}$ and the transformed Hamiltonian

$$G_{Yn}^i = \partial_j S_n J_0^{ji}, (n = 1, 2) \tag{19a}$$

$$\bar{H}_1 = H_{A1} - \boldsymbol{G}_{Y1} \cdot dH_{A0} - \partial_t S_1, \tag{19b}$$

$$\begin{aligned} \bar{H}_2 = H_{A2} - \boldsymbol{G}_{Y1} \cdot dH_{A1} + \frac{1}{2} \boldsymbol{G}_{Y1} \cdot d(\boldsymbol{G}_{Y1} \cdot dH_{A0}) \\ - \boldsymbol{G}_{Y2} \cdot dH_{A0} - \partial_t S_2 \end{aligned} \tag{19c}$$

For the usual GY Lie-transform, the $\bar{H}_n$ s are chosen to be independent of gyroangle ξ, and the ξ dependent part is transformed into S_n

$$\partial_t S_n + \{S_n, \bar{H}_n\} = \widetilde{\delta\Psi}_n \tag{20}$$

with $\widetilde{\delta\Psi}_n \equiv \delta\Psi_n - \langle\delta\Psi_n\rangle$,

$$\delta\Psi_1 = H_{A1} = \delta\phi - \delta\boldsymbol{A}\cdot(\dot{\boldsymbol{X}} + \dot{\boldsymbol{\rho}}_0), \tag{21a}$$

$$\delta\Psi_2 = H_{A2} - \frac{1}{2}G^i_{Y1}\partial_i(H_{A1} + \bar{H}_1), \tag{21b}$$

with $\langle\cdot\rangle$ denoting the gyrophase averaging. Note that the secularity problem is avoided when the gauge functions are chosen in this way.[21] Solving the equations above, we can obtain S_n

$$(\dot{S}_1)_0 \equiv \frac{d_0 S_1}{dt} = \widetilde{H_{A1}}, \tag{22a}$$

$$\frac{d_0 S_2}{dt} = \widetilde{H_{A2}} - G^i_{Y1}\partial_i\bar{H}_1 - \frac{1}{2}\widetilde{\left\{S_1, (\dot{S}_1)_0\right\}}, \tag{22b}$$

$$\frac{d_0}{dt} \equiv \partial_t + \dot{\boldsymbol{X}}_0\cdot\nabla + \dot{v}_{\parallel 0}\partial_{v_\parallel} + \dot{\xi}_0\partial_\xi. \tag{22c}$$

Then, using Eq. (19), we have

$$G^{\boldsymbol{X}}_{Yn} = -\frac{\boldsymbol{b}_0}{B^*_{\parallel 0}}\times\nabla S_n - \partial_{v_\parallel}S_n\frac{\boldsymbol{B}^*_0}{B^*_{\parallel 0}}, \tag{23a}$$

$$G^{v_\parallel}_{Yn} = \frac{\boldsymbol{B}^*_0}{B^*_{\parallel 0}}\cdot\nabla S_n, \tag{23b}$$

$$G^{\xi}_{Yn} = -\partial_\mu S_n, \tag{23c}$$

$$G^{\mu}_{Yn} = \partial_\xi S_n, (n = 1, 2). \tag{23d}$$

Note that the generating vector fields satisfy $\langle G^i_{Yn}\rangle = 0$. The transformed Hamiltonian is obtained by gyro-averaging of Eqs. (19b) and (19c)

$$\bar{H}_1 = \langle H_{A1}\rangle = \langle\delta\phi\rangle - \dot{\boldsymbol{X}}_0\cdot\langle\delta\boldsymbol{A}\rangle - \dot{\xi}_0\langle\delta\boldsymbol{A}\cdot\partial_\xi\boldsymbol{\rho}_0\rangle, \tag{24a}$$

$$\bar{H}_2 = \frac{1}{2}\langle\delta\boldsymbol{A}^2\rangle - \frac{1}{2}\left\langle\left\{S_1, (\dot{S}_1)_0\right\}\right\rangle, \tag{24b}$$

which are the same as the previous results.[7,23,24] Note that the second-order Hamiltonian can be written explicitly as[6]

$$\bar{H}_2 = \frac{1}{2}\langle\delta\boldsymbol{A}^2\rangle - \frac{1}{2B}\left\langle\frac{\partial}{\partial\bar{\mu}}(\dot{S}_1)_0^2 + \frac{1}{B}\bar{\nabla}S_1\cdot\boldsymbol{b}\times\bar{\nabla}(\dot{S}_1)_0\right\rangle. \tag{25}$$

Here, we make some discussions about Eq. (25).

(1) In the long-wave-length limit, Eq. (25) becomes

$$\bar{H}_2 = \frac{1}{2}\langle\delta\boldsymbol{A}^2\rangle - \frac{1}{2B}\left\langle\frac{\partial}{\partial\bar{\mu}}(\dot{S}_1)_0^2\right\rangle, \tag{26}$$

considering the ordering

$$\frac{\frac{1}{B}\bar{\nabla}S_1\cdot\boldsymbol{b}\times\bar{\nabla}(\dot{S}_1)_0}{\frac{\partial}{\partial\bar{\mu}}(\dot{S}_1)_0^2} \sim \frac{k_\perp^2 S_1(\dot{S}_1)_0/B}{(\dot{S}_1)_0^2/\mu} \sim \frac{k_\perp^2\rho^2\mu}{\rho^2 B} \sim (k_\perp\rho)^2, \tag{27}$$

with $\boldsymbol{k}_\perp$ the perpendicular wave vector and ρ the gyroradius. According to Eqs. (21a) and (22a), up to $\mathcal{O}(k_\perp\rho)$, $(\dot{S}_1)_0$ can be explicitly written as

$$(\dot{S}_1)_0 = \boldsymbol{\rho}\cdot\nabla(\delta\phi_c - \dot{\boldsymbol{X}}\cdot\delta\boldsymbol{A}_c) - \dot{\boldsymbol{\rho}}\cdot\delta\boldsymbol{A}_c - \boldsymbol{\rho}\cdot\widetilde{(\boldsymbol{\rho}\cdot\nabla)}\delta\boldsymbol{A}_c, \tag{28}$$

where the subscript c means evaluating at the guiding center. Then, the last term in Eq. (26) is

$$\begin{aligned}\frac{1}{2B}\left\langle\frac{\partial}{\partial\bar{\mu}}(\dot{S}_1)_0^2\right\rangle = \frac{1}{2}\left[\delta\boldsymbol{A}^2_{c\perp} + \left(\frac{\boldsymbol{b}_0\times\nabla(\delta\phi_c - \dot{\boldsymbol{X}}\cdot\delta\boldsymbol{A}_c)}{B}\right)^2\right]\\ + \frac{1}{2}\left[2\delta\boldsymbol{A}_c\cdot\frac{\boldsymbol{b}_0\times\nabla(\delta\phi_c - \dot{\boldsymbol{X}}\cdot\delta\boldsymbol{A}_c)}{B}\right.\\ \left. + \frac{\mu}{B}(\partial_1\delta A_{c1} - \partial_2\delta A_{c2})^2\right]\end{aligned} \tag{29}$$

with $(\hat{2}, \hat{1}, \boldsymbol{b})$ form a right-handed frame. Similar analysis as Eq. (27), the ordering in Eq. (29) respect to $\delta\boldsymbol{A}^2_{c\perp}$ is $(1, (k_\perp\rho)^2\left(\frac{\rho}{R}\right)^2, (k_\perp\rho)\frac{\rho}{R}, (k_\perp\rho)^2)$, where we have used $|\frac{\nabla(\dot{\boldsymbol{X}}\cdot\delta\boldsymbol{A}_c)/B}{\delta\boldsymbol{A}_{c\perp}}| \sim \frac{k_\perp v_D}{B} \sim k_\perp\frac{\rho v_\parallel}{RB} \sim \frac{\rho}{R}(k_\perp\rho)$ and R is the major radius of a tokamak. According to Eqs. (24), (26), and (29), up to $\mathcal{O}(\epsilon_\delta^2)$ the gyrokinetic Hamiltonian can be written as

$$\bar{H} = \frac{1}{2}\left(\overline{v_\parallel} - \delta A_\parallel(\bar{\boldsymbol{X}}, t)\right)^2 + \bar{\mu}\left[B + \delta B_\parallel(\bar{\boldsymbol{X}}, \boldsymbol{t})\right] + \delta\phi(\bar{\boldsymbol{X}}, t). \tag{30}$$

It is useful to compare Eq. (30) with the previous[7] gyro-center Hamiltonian [their Equation (20)], which is written as

$$\bar{H} = \frac{1}{2}\left(\overline{v_\parallel}\boldsymbol{b}_0 - \delta\boldsymbol{A}(\bar{\boldsymbol{X}}, t)\right)^2 + \bar{\mu}\left[B + \delta B_\parallel(\bar{\boldsymbol{X}}, \boldsymbol{t})\right] + \delta\phi(\bar{\boldsymbol{X}}, t). \tag{31}$$

It is $\delta A_\parallel(\bar{\boldsymbol{X}}, t)$ instead of $\delta\boldsymbol{A}(\bar{\boldsymbol{X}}, t)$ that should be used in the gyro-center Hamiltonian, for any vector potential perturbation. The point is that the term $\langle\{,\}\rangle$ in Eq. (24b) was ignored in Ref. 7 by taking it as a higher order term relative to $\frac{1}{2}\langle\delta\boldsymbol{A}^2\rangle$, however, the order of the $\langle\{,\}\rangle$ term is the same as the $\frac{1}{2}\langle\delta\boldsymbol{A}^2\rangle$ term, which follows from Eq. (29). The difference between Eqs. (30) and (31) can affect the particles orbits in a strong $\delta\boldsymbol{A}_\perp$ perturbation field, and the numerical example will be shown in Sec. IV C. Eq. (30) can be easily understood from the scalar invariance, and the detailed discussion will be shown latter.

(2) Due to the electromagnetic gauge invariance,[18,44] the perturbation $(\delta\phi, \delta\boldsymbol{A})$ can be transformed as $(\delta\phi^*, \delta A_\parallel)$; Eq. (29) becomes

$$\frac{1}{2B}\left\langle\frac{\partial}{\partial\bar{\mu}}(\dot{S}_1)_0^2\right\rangle = \frac{1}{2}\left(\frac{\boldsymbol{b}_0\times\nabla(\delta\phi_c^* - v_\parallel\delta A_{c\parallel})}{B}\right)^2, \tag{32}$$

with $\bar{H}_1 = \langle\delta\phi^* - v_\parallel\delta A_\parallel\rangle$, then the second-order Hamiltonian becomes

$$\bar{H}_2 = \frac{1}{2}\langle\delta A^2_\parallel\rangle - \frac{1}{2}\left(\frac{\boldsymbol{b}_0\times\nabla(\delta\phi_c^* - v_\parallel\delta A_{c\parallel})}{B}\right)^2, \tag{33}$$

so that the second-order Hamiltonian, in the long-wave-length limit, will be simply written as $\bar{H}_2 = \frac{1}{2}\delta A^2_{c\parallel}$ with the

$\mathcal{O}((k_\perp\rho)^2\epsilon_\delta^2)$ term ignored. The second term in Eq. (33) can be ignored in the long-wave-length limit, which is a good approximation for toroidal-field-ripple perturbation discussed in this paper. However, for a general perturbation, this term should be retained.

Eq. (33) can be written as an alternative form

$$\bar{H}_2 = \frac{1}{2}\langle \delta A_\parallel^2\rangle - \frac{1}{2}\langle \boldsymbol{v}_{1\perp}^2\rangle, \tag{34a}$$

$$\boldsymbol{v}_{1\perp} = \{\boldsymbol{\rho}, H_1\}, \tag{34b}$$

which may be useful for readers. The brief proof of Eq. (34a) is as follows:

$$\begin{aligned}\langle \boldsymbol{v}_{1\perp}^2\rangle &= \langle(\partial_\xi\boldsymbol{\rho}\partial_\mu H_1 - \partial_\mu\boldsymbol{\rho}\partial_\xi H_1)^2\rangle \\ &= \left\langle \rho^2\left(\partial_\mu\widetilde{H}_1\right)^2 + \left(\frac{\rho}{2\mu}\right)^2\left(\partial_\xi\widetilde{H}_1\right)^2\right\rangle \\ &\simeq \frac{\rho^2}{4\mu^2}\left\langle \widetilde{H}_1^2 + \left(\partial_\xi\widetilde{H}_1\right)^2\right\rangle \\ &= \left(\frac{\boldsymbol{b}_0\times\nabla\left(\delta\phi_c^* - v_\parallel\delta A_{c\parallel}\right)}{B}\right)^2,\end{aligned} \tag{35}$$

where we have used $\widetilde{H}_1 \simeq \boldsymbol{\rho}\cdot\nabla(\delta\phi_c^* - v_\parallel\delta A_{c\parallel})$, with an $\mathcal{O}((k_\perp\rho)^2)$ term ignored.

To end this section, we present the understanding of Eq. (30) from the point view of scalar invariance. According to Eq. (15d), the last term in Eq. (24a) can be written as

$$-\dot{\xi}_0\langle\delta\boldsymbol{A}\cdot\partial_\xi\boldsymbol{\rho}_0\rangle = \langle -G_{A1}^\mu\cdot B\rangle \approx \mu\langle\delta B_\parallel\rangle, \tag{36}$$

then Eq. (24a) becomes

$$\bar{H}_1 = \langle H_{A1}\rangle = \langle\delta\phi\rangle - \dot{\boldsymbol{X}}_0\cdot\langle\delta\boldsymbol{A}\rangle + \mu\langle\delta B_\parallel\rangle, \tag{37}$$

which clearly shows that, according to the scalar invariance, it is $G_{\boldsymbol{A}1}^\mu$, the first-order change of the magnetic moment, that results to the last term of $\bar{H}_1$. The second-order term $\langle\{,\}\rangle$ in Eq. (24b) was previously ignored[7] by taking it as a higher order term relative to $\frac{1}{2}\langle\delta\boldsymbol{A}^2\rangle$. However, analyzing the $\langle\{,\}\rangle$ term in detail, we found that this term reduces to $\langle\delta\boldsymbol{A}_\perp^2\rangle$, which cancels the perpendicular part in the term $\frac{1}{2}\langle\delta\boldsymbol{A}^2\rangle$. This result can also be obtained from Eq. (19), and the detailed analysis is as follows.

By using Eq. (19b), the second term on the left side of Eq. (19c) can be written as

$$\begin{aligned}-\boldsymbol{G}_{Y1}\cdot d\boldsymbol{H}_{A1} &= -\boldsymbol{G}_{Y1}\cdot d(\bar{H}_1 + \boldsymbol{G}_{Y1}\cdot d\bar{H}_0 + \partial_t S_1) \\ &\approx -\boldsymbol{G}_{Y1}\cdot d\bar{H}_1 - \boldsymbol{G}_{Y1}\cdot d(\boldsymbol{G}_{Y1}\cdot d\boldsymbol{H}_{A0}),\end{aligned} \tag{38}$$

where we have used the low frequency approximation $\frac{\omega}{\Omega}\ll 1$, with Ω the gyro-frequency. Note that $\langle -\boldsymbol{G}_{Y1}\cdot d\bar{H}_1\rangle = 0$. Then, substituting Eq. (38) into Eq. (19c) and gyro-averaging it, we have

$$\bar{H}_2 = \langle H_{A2}\rangle - \left\langle\frac{1}{2}\boldsymbol{G}_{Y1}\cdot d(\boldsymbol{G}_{Y1}\cdot d\boldsymbol{H}_{A0})\right\rangle. \tag{39}$$

The term $\langle\frac{1}{2}\boldsymbol{G}_{Y1}\cdot d(G_{Y1}\cdot d\bar{H}_{A0})\rangle$ can be written as

$$\begin{aligned}\left\langle\frac{1}{2}\boldsymbol{G}_{Y1}\cdot d(\boldsymbol{G}_{Y1}\cdot d\bar{H}_{A0})\right\rangle &= \frac{1}{2}\langle\partial_{\boldsymbol{Z}}\cdot(\boldsymbol{G}_{Y1}\boldsymbol{G}_{Y1}\cdot\partial_{\boldsymbol{Z}}H_{A0})\rangle \\ &\approx \frac{1}{2}\left\langle\left[\partial_\mu\left(G_{Y1}^\mu G_{Y1}^\mu B\right) + \partial_\xi\left(G_{Y1}^\xi G_{Y1}^\mu B\right)\right]\right\rangle \\ &= \langle G_{Y1}^\mu\partial_\mu G_{Y1}^\mu B\rangle,\end{aligned} \tag{40}$$

where we have used the fact that $\boldsymbol{G}_1$ is an incompressible flow in the phase space $\frac{1}{\mathcal{J}}\partial_i(\mathcal{J}G_1^i) = 0$,[19,24] and the approximation $\boldsymbol{G}_n \approx \boldsymbol{G}_n(\mu,\xi)$.

Considering the ordering in Eq. (22c), one finds

$$\frac{\partial_t}{\dot{\xi}_0\partial_\xi} \sim \frac{\dot{v}_{\parallel 0}\partial_{v_\parallel}}{\dot{\xi}_0\partial_\xi} \sim \frac{\omega}{\Omega}, \tag{41a}$$

$$\frac{\dot{\boldsymbol{X}}_0\cdot\nabla}{\dot{\xi}_0\partial_\xi} \sim \frac{v_\parallel\nabla_\parallel + v_D\nabla_\perp}{\Omega} \sim \rho\nabla_\parallel + \frac{\rho}{R}\rho\nabla_\perp \sim \frac{\rho}{R} + \frac{\rho}{R}(k_\perp\rho) \sim \frac{\rho}{R}. \tag{41b}$$

Therefore, we have $\frac{d_0}{dt} \approx \dot{\xi}_0\partial_\xi = \Omega\partial_\xi$ with the low frequency approximation $\frac{\omega}{\Omega}$.[7] Then following Eqs. (20) and (22), we have $\dot{S}_1 \approx -\delta\boldsymbol{A}_c\cdot\dot{\boldsymbol{\rho}}_0$ in the long-wave-length limit; therefore, $S_1 \approx -\boldsymbol{\rho}_0\cdot\delta\boldsymbol{A}_c$ and

$$G_{Y1}^\mu = \partial_\xi S_1 \approx -\partial_\xi\boldsymbol{\rho}_0\cdot\delta\boldsymbol{A}_c, \tag{42a}$$

$$\partial_\mu G_{Y1}^\mu \approx -\partial_\mu(\partial_\xi\boldsymbol{\rho}_0)\cdot\delta\boldsymbol{A}_c = -\frac{1}{2\mu}\partial_\xi\boldsymbol{\rho}_0\cdot\delta\boldsymbol{A}_c. \tag{42b}$$

Subsisting Eq. (42) into Eq. (40), we can obtain

$$\begin{aligned}\left\langle\frac{1}{2}\boldsymbol{G}_{Y1}\cdot d(\boldsymbol{G}_1\cdot d\bar{H}_{A0})\right\rangle &= \langle G_{Y1}^\mu\partial_\mu G_{Y1}^\mu\cdot B\rangle \\ &\approx \frac{B}{2\mu}\langle(\partial_\xi\boldsymbol{\rho}_0\cdot\delta\boldsymbol{A}_c)^2\rangle \\ &= \frac{1}{2}\delta\boldsymbol{A}_{c\perp}^2.\end{aligned} \tag{43}$$

Eqs. (43) and (39) show that there is no $\delta\boldsymbol{A}_\perp^2$ term in the second-order transformed Hamiltonian. And, in a Hamiltonian system with only magnetic perturbation $\delta\boldsymbol{A}$, according to Eqs. (18), (39), and (43), the second-order Hamiltonian in the drift kinetic approximation becomes

$$\bar{H}_2 \approx \frac{1}{2}\delta A_{c\parallel}^2. \tag{44}$$

Note that the main term in the second order of transformed Hamiltonian is the parallel part even considering the full magnetic perturbation.

According to the scalar invariance, the result is easily to be understood in the two-step transform. Eqs. (19), (39), and (43) clearly show that for the purpose of searching a new constant magnetic moment, we make the gyrocenter transform; it is $\frac{1}{2}G_{Y1}^i\partial_i G_{Y1}^\mu$, the second-order change of the magnetic moment, that cancels the $\delta A_\perp^2$. The same result can be obtained by using the conventional one-step transform; since the equivalence between the two-step and the one-step transforms has been rigorously proved in the Appendix in Ref. 24, we ignore the detailed discussion on the one-step transform here.

C. The I-transform

The I-transform is a method to solve the equations of motion, which can decouple the unperturbed motion from the perturbed motion.[19–21] That means we find a new coordinates $\boldsymbol{Z}_I$, in which the perturbation part of the Hamiltonian is transformed away. In brief, the form of the Hamiltonian in $\boldsymbol{Z}_I$ is the same as the unperturbed one H_0. T_I stands for the transform from $\bar{\boldsymbol{Z}}$ to $\boldsymbol{Z}_I$, and then the transform relations are

$$G^i_{In} = \partial_j S_n J^{ji}_0, (n = 1, 2), \tag{45a}$$

$$0 = \bar{H}_1 + \bar{H}_2 - G^i_{I1}\partial_i \bar{H}_0 - \partial_t S_1, \tag{45b}$$

$$0 = -G^i_{I1}\partial_i(\bar{H}_1 + \bar{H}_2) + \frac{1}{2}G^i_{I1}\partial_i\left(G^j_{I1}\partial_j \bar{H}_0\right) - G^i_{I2}\partial_i \bar{H}_0 - \partial_t S_2. \tag{45c}$$

The gauge functions are

$$\frac{d_0 S_1}{dt} = \delta\bar{H} = \bar{H}_1 + \bar{H}_2, \tag{46a}$$

$$\frac{d_0 S_2}{dt} = -\frac{1}{2}\{S_1, \delta\bar{H}\}. \tag{46b}$$

And, the transformed equations of motion are

$$\frac{d_0 Z^i_I}{dt} = J^{ij}_0 \partial_j H_0, \tag{47}$$

which clearly shows that they are the same as the unperturbed ones.

IV. NLT SIMULATION OF THE GUIDING CENTER ORBIT IN RIPPLE FIELD

A. The code NLT

The code NLT, based on the I-transform method, is developed to compute the GC orbit.[24] NLT treats the electromagnetic potential perturbation $(\delta\phi, \delta\boldsymbol{A})$ directly rather than the field $(\delta\boldsymbol{E}, \delta\boldsymbol{B})$, and NLT can compute the GC orbit in any given perturbation field. The long time computation of the orbit is decomposed to many short-time I-transforms. The main procedure to push forward the orbit of a particle in every time step contains the three kinds of transform presented in Sec. III.

The procedure decomposes as follows: first, we do the $\delta\boldsymbol{A}$ transform to make the magnetic perturbation appear in the Hamiltonian in the coordinates $\boldsymbol{Z}_A$, do the gyrocenter transform to find the invariant GY magnetic moment in $\bar{\boldsymbol{Z}}$, and then use the I-transform method to find the new coordinates $\boldsymbol{Z}_I$, in which the equations of motion is the same as the unperturbed ones; finally, we use the fourth-order Runge-Kutta method to evolve the equations to get the GY position in phase space $\boldsymbol{Z}_I$ of the next time step. Then, the inverse I-transform is used to get the real GY orbit. The excursion of the orbit between the unperturbed one and the real one is presented by the generating vector of the inverse I-transform. The inverse GY transform and the inverse $\delta\boldsymbol{A}$ transform are used successively to obtain the position of the next time step in coordinates $\boldsymbol{Z}_A$ and $\boldsymbol{Z}$. To

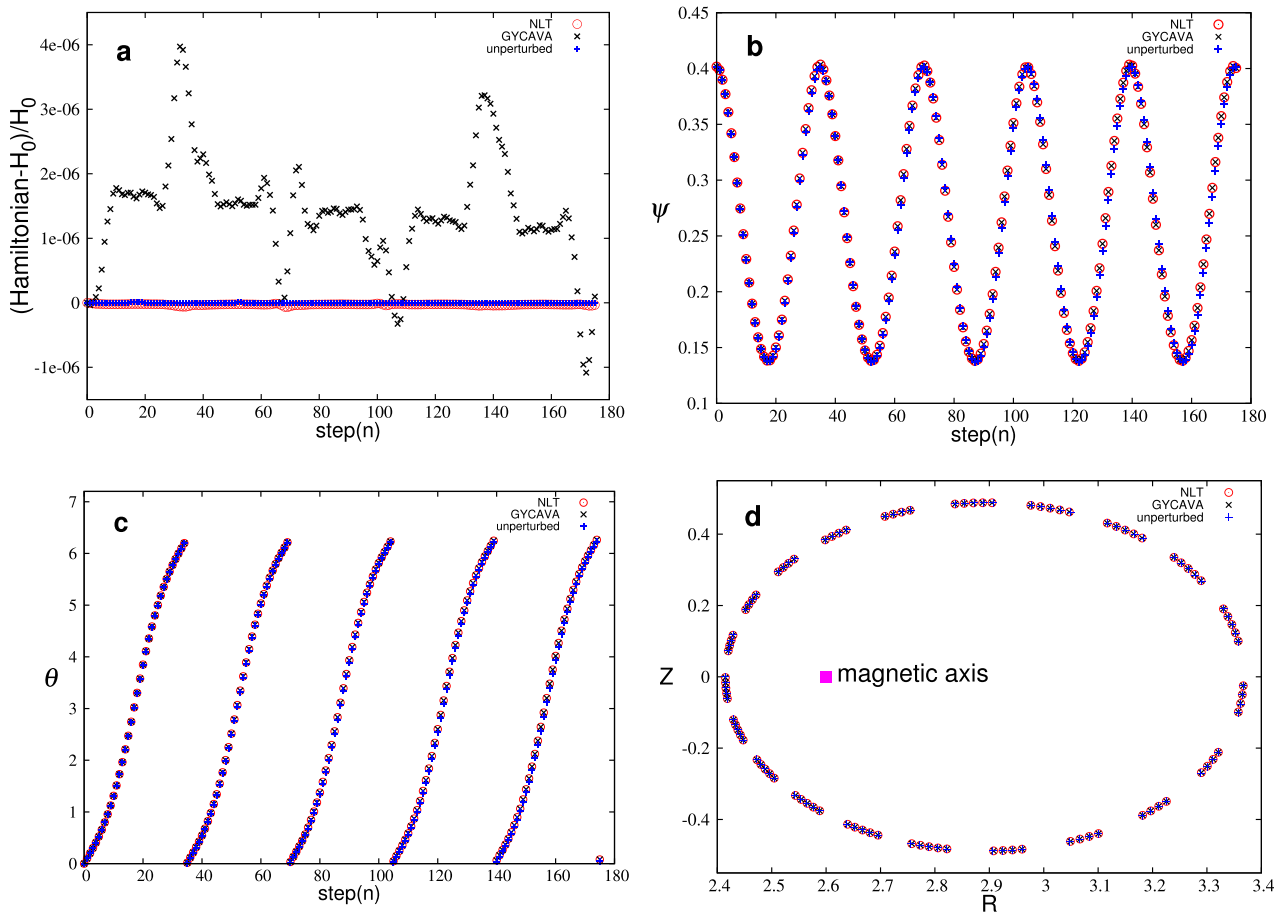

FIG. 1. Passing particle with $\frac{v_\parallel}{v} = 0.8$ launched from $(R = 3.367\,\mathrm{m}, \theta = 0, \zeta = 0)$. (a): Energy evolution. (b): The radial evolution. (c): θ (modulo 2π) evolution. (d): The Poincare section plots.

validate the results of NLT, which is based on the two-step transform used in this paper, the code GYCAVA,[22] which is based on the conventional one-step Lie-transform perturbation method, is used as a benchmark in the numerical examples in Sec. IV C.

B. The vector potential δA corresponding to the ripple field

The main effect of the ripple field in a tokamak is the perturbation of the toroidal magnetic field strength, which can be simply written as

$$\delta B_T = \delta(\Psi,\theta)B_0\cos(N\zeta), \tag{48}$$

where Ψ is the poloidal magnetic flux, θ and ζ are the poloidal angle and toroidal angle, respectively, and N is the number of the toroidal field coils. The corresponding magnetic potential in the magnetic coordinate is chosen as

$$\delta\boldsymbol{A} = \delta A_\theta(\Psi,\theta,\zeta)\nabla\theta. \tag{49}$$

Using $\delta B_T = R\nabla\zeta\cdot\nabla\times\delta\boldsymbol{A}$, we have

$$\delta B_T = \mathcal{J}^{-1}R\partial_\Psi\delta A_\theta, \tag{50}$$

with the Jacobian $\mathcal{J}^{-1} = \nabla\Psi\times\nabla\theta\cdot\nabla\zeta$. Combining with Eq. (48), we can obtain

$$\delta A_\theta(\Psi,\theta,\zeta) = \int_0^\Psi \frac{\mathcal{J}}{R}\delta(\Psi',\theta)B_0\cos(N\zeta)d\Psi'. \tag{51}$$

The $\delta\boldsymbol{A}$ chosen in this way ensures the main effect of the ripple field and naturally guarantees the zero divergence of the perturbation magnetic field $\delta\boldsymbol{B}$. The main parameters of the equilibrium in TFTR are the plasma major radius $R_0 = 2.60\,\mathrm{m}$, minor radius $a = 0.95\,\mathrm{m}$, plasma current $I_p = 1.4\,\mathrm{MA}$, and the toroidal magnetic field at magnetic axis $B_T = 4.0\,\mathrm{T}$. The current profile is modelled by a simple parabolic $J(r) = J_0(1-\frac{r^2}{a^2})^2$, and the ripple magnitude is taken from a fit[32] to the calculated vacuum ripple which is modelled by

$$\delta = \delta_0\exp\left\{\frac{\left[(R_0+r\cos\theta-R_{rip})^2+b_{rip}(r\sin\theta)^2\right]^{1/2}}{W_{rip}}\right\}, \tag{52}$$

where $R_{rip} = 2.25\,\mathrm{m}$ is the major radius of the "center" of the ripple, $b_{rip} = 1.1$ is the ellipticity, $W_{rip} = 0.185\,\mathrm{m}$ is the ripple scale length, and $\delta_0 = 1.4\times10^{-5}$.[34] The code "shafranov" developed by Xiao,[45] which has been used in GYCAVA and NLT,[22,24] is used to prepare the equilibrium data of TFTR.

C. The guiding-center orbit in ripple field in TFTR

Numerical results of the GC-orbit of 3.5 MeV alpha particles are shown in Figs. 1–3. Figs. 1(a), 2(a), and 3(a) show

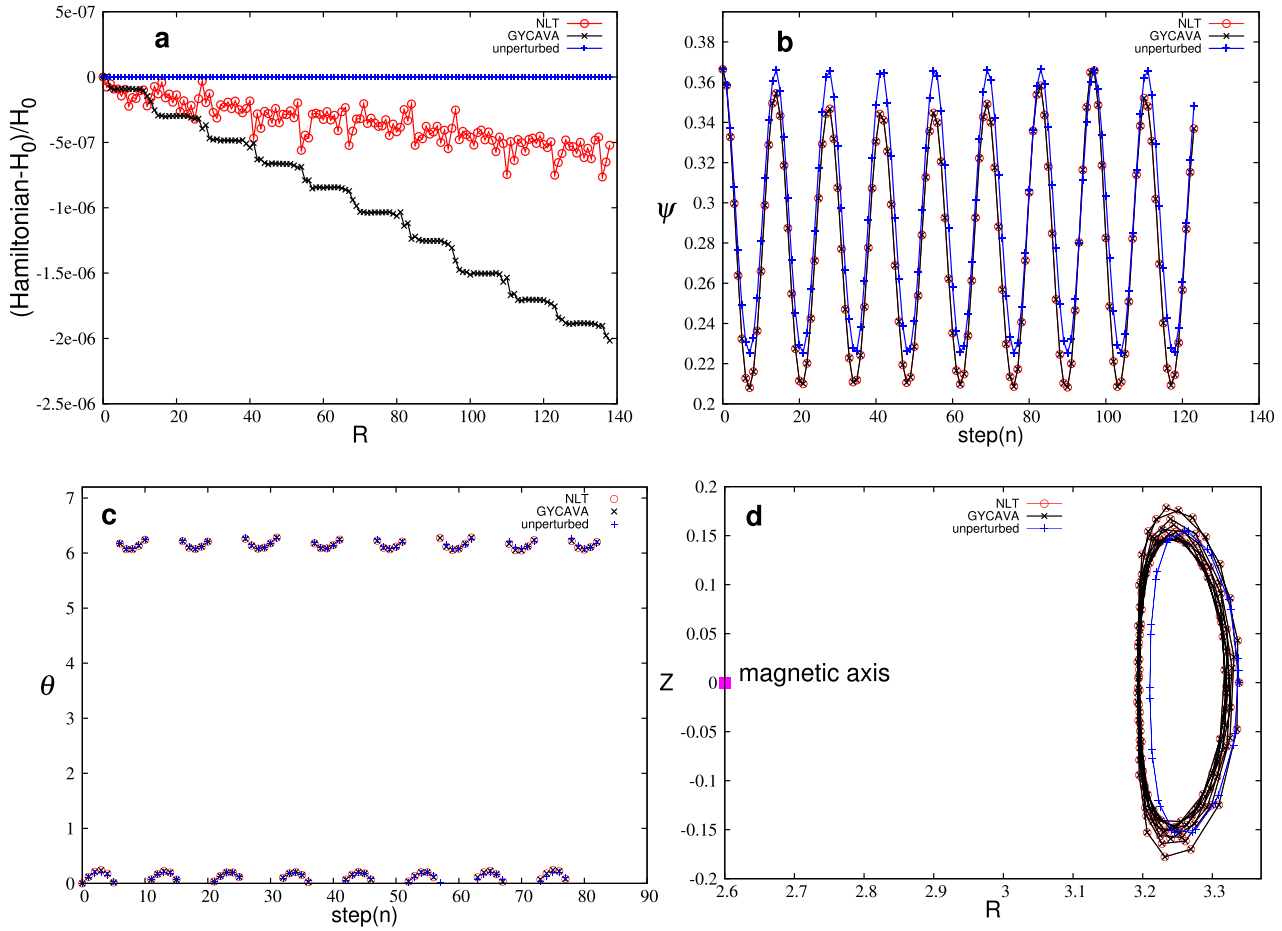

FIG. 2. Trapped particle with $\frac{v_\parallel}{v} = 0.2$ launched from $(R = 3.338\,\mathrm{m}, \theta = 0, \zeta = 0)$. (a): Energy evolution. (b): The radial evolution. (c): θ (modulo 2π) evolution. (d): Orbit projected on the minor cross section.

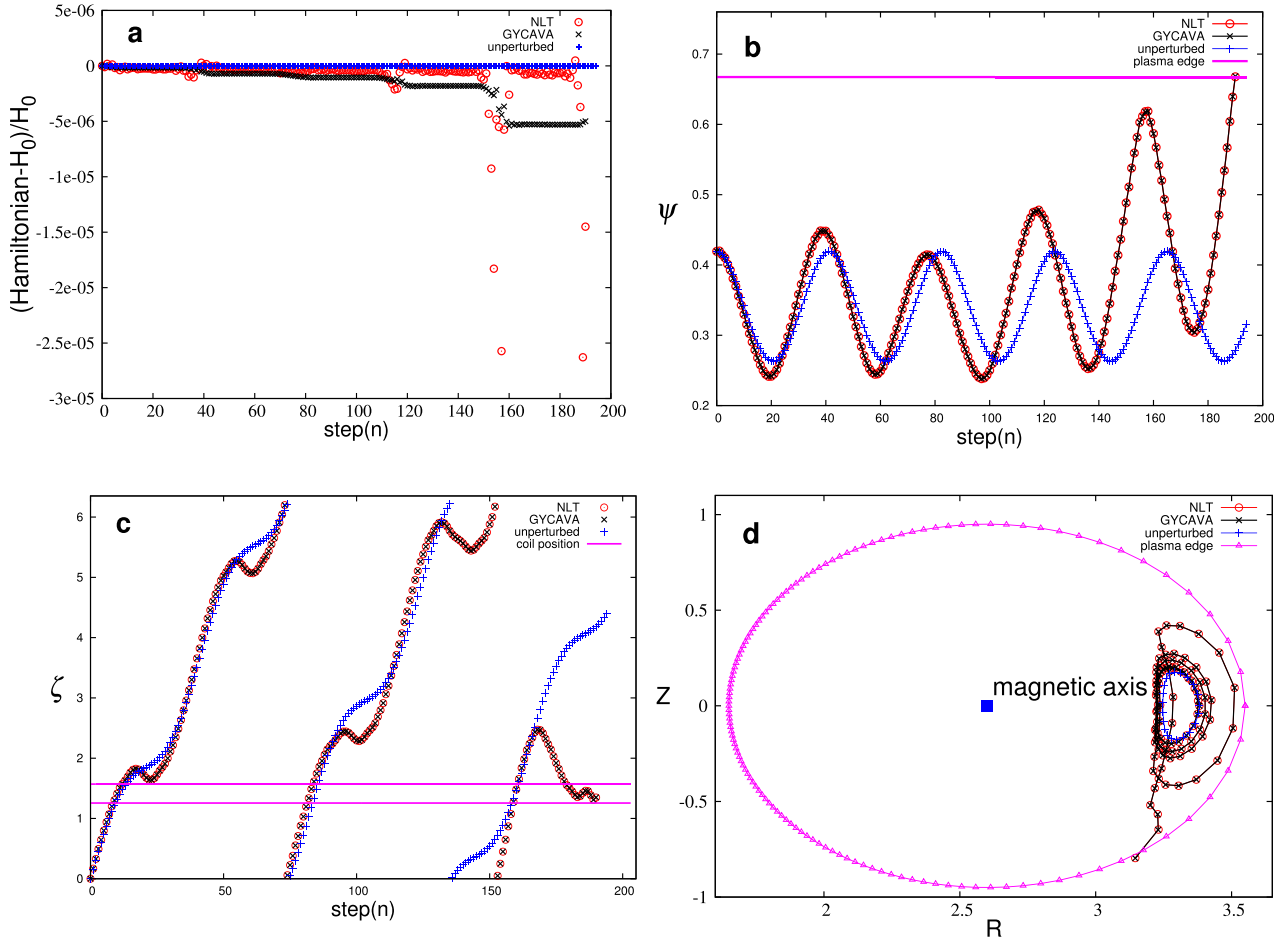

FIG. 3. Trapped particle with $\frac{v_\parallel}{v} = 0.2$ launched from $(R = 3.381\text{m}, \theta = 0, \zeta = 0)$. (a): Energy evolution. (b): The radial evolution. (c): ζ (modulo 2π) evolution. The two horizontal lines indicate the position of the two toroidal field coils. (d): Orbit projected on the minor cross section.

that the energy conservation is good for both NLT and GYCAVA codes. It is shown in Fig. 1 that the ripple field has little effect on passing particles. Figs. 2 and 3 indicate that the toroidal ripple field may induce radial stochastic diffusion of trapped energetic alpha particles. Fig. 3(c) shows that the toroidal angle ζ of the locally trapped particle keeps in the middle of two toroidal field coils, which means that the particle is eventually trapped in the ripple magnetic field well.

Fig. 4 shows the effect on the orbit due to the difference between Eqs. (30) and (31). It is shown in Fig. 4 that the two equations give the same orbits in weak $\delta \boldsymbol{A}_\perp$ perturbation field, when the particles are near the plasma edge, where the $\delta \boldsymbol{A}_\perp$ perturbation is strong, the orbits are notably different.

D. Verification of GWB's criterion

The criterion δ_s for the ripple stochasticity is theoretically given by Goldston, White, and Boozer[30] as

$$\delta_s = \left[\frac{\epsilon}{N\pi q}\right]^{3/2} \frac{1}{\rho q'}, \tag{53}$$

with ϵ the local inverse aspect ratio, which has been verified by Tani via using an orbit-following Monte-Carlo code.[31] Fig. 5 briefly shows the criterion, the outmost circle is the plasma edge and the inner circle is given by Eq. (53). If a banana tip is located outside the inner circle, it shall be stochastic; therefore, the inner circle shall be referred to as the critical curve. Particle 3 runs stochastic orbit for its bounce point is out of the inner circle, and particle 1 runs nonstochastic orbit for its banana tip is inside of the inner circle. If the ripple field strength becomes stronger, then the critical curve shrinks, and the stochastic area is larger, in that case particle 1 may run stochastic orbit. This is the method we use to verify the theoretical formula.

As is shown in Fig. 6, 9 alpha particles, with the same $\frac{v_\parallel}{v} = 0.2$ and energy $E = 3.5\,\text{MeV}$, are launched from different major radius in the out middle plane. We observe the property of the orbits to find the critical major radius to compare with the theoretical one. Fig. 6 shows 4 different amplitude of the ripple field $\delta_0 = (0.7, 1.4, 2.8, 4.2) \times 10^{-5}$, and TFTR's parameter is $\delta_0 = 1.4 \times 10^{-5}$. The numerical results denoted by the dashed line are consistent with the theoretical result denoted by the solid line. The difference between the numerical results and the theoretical one may be due to the large banana width of the alpha particles.

V. SUMMARY

In conclusion, in the nonlinear gyrokinetic equation for magnetic potential perturbation, the main term of the

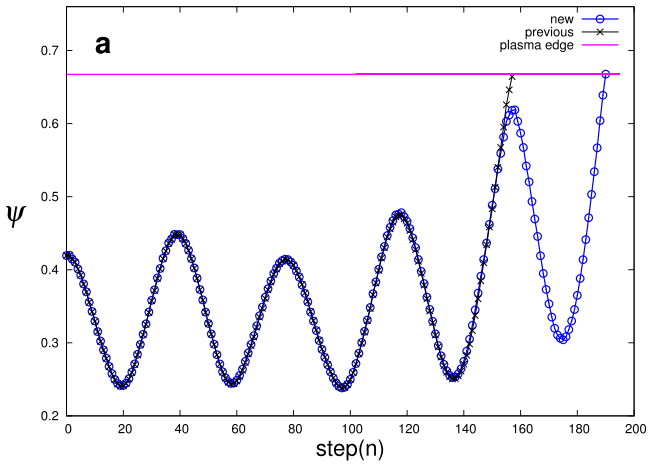

FIG. 4. Difference between orbits computed by using Eqs. (30) and (31). Trapped particle with $\frac{v_\parallel}{v} = 0.2$ launched from $(R = 3.381\,\mathrm{m}, \theta = 0, \zeta = 0)$. "New" and "previous" indicate the orbits given by Eqs. (30) and (31), respectively. (a): The radial evolution. (b): Orbits projected on the minor cross section.

second-order transformed Hamiltonian is $\frac{1}{2}\delta A_\parallel^2$ for any magnetic perturbation in the long-wave-length limit. This result can be easily understood in the two-step transform, that it is the little change of the magnetic moment that transforms

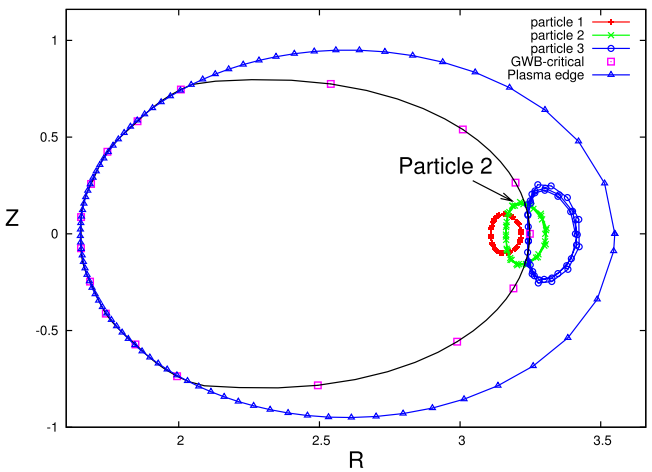

FIG. 5. The criterion given by GWB. The outmost circle is the plasma edge, and the inner circle is the critical curve given by GWB's formula. Three banana-like curves are the orbit of three particles with the same $\frac{v_\parallel}{v} = 0.2$, $\theta = 0, \zeta = 0$ launched from different R.

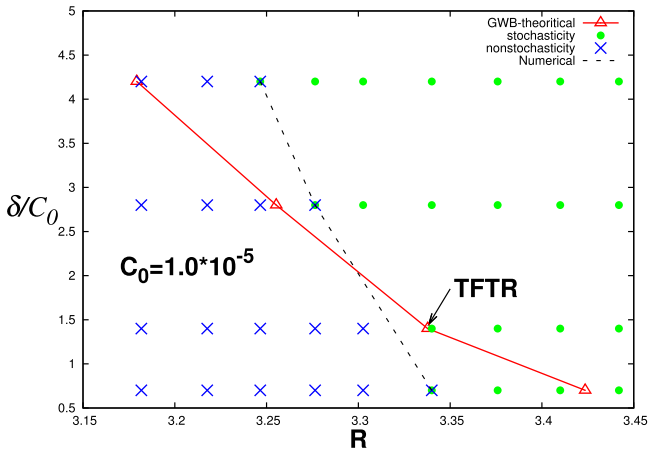

FIG. 6. Collisionless stochastic loss region in space of ripple field amplitude and initial major radius. Particles launched from the middle plane with the same pitch = 0.2. Particles run the stochastic orbit are shown by solid points and the nonstochastic are shown by crosses. Solid line is the theoretical result, and the dashed line is the numerical result.

away the $\frac{1}{2}\delta A_\perp^2$ part, as is shown in Eq. (43); this is different from the result expected previously.[7]

The code NLT is improved to compute the guiding center orbit in the ripple field in TFTR. We have included the second-order Hamiltonian in the long-wave-length limit, which was ignored in most of the previous simulation works on the effect of ripple field. If we used the second-order Hamiltonian given in Ref. 7, the alpha particle orbit in the ripple field would be significantly changed, as is shown in Fig. 4. However, when the corrected second-order Hamiltonian is included, the numerical results indicate that there is little effect of the second-order Hamiltonian ($\frac{1}{2}\delta A_\parallel^2$) on the alpha particle orbit in the ripple field.

The improved NLT is used to verify the ripple stochastic diffusion criterion, the result agrees well with the GWB model, and the difference between our numerical results and the GWB model may be due to the large orbit width of the alpha particle, which shall be left as a topic in future researches.

ACKNOWLEDGMENTS

This work was supported by the National Natural Science Foundation of China under Grant Nos. 11375196 and 11405174 and the National ITER program of China under Contract No. 2014GB113000.

[1]T. M. Antonsen, Jr. and B. Lane, Phys. Fluids **23**, 1205 (1980).
[2]P. J. Catto, W. M. Tang, and D. E. Baldwin, Plasma Phys. **23**, 639 (1981).
[3]E. A. Frieman and L. Chen, Phys. Fluids **25**, 502 (1982).
[4]D. H. E. Dubin, J. A. Krommes, C. Oberman, and W. W. Lee, Phys. Fluids **26**, 3524 (1983).
[5]T. S. Hahm, Phys. Fluids **31**, 2670 (1988).
[6]T. S. Hahm, W. W. Lee, and A. Brizard, Phys. Fluids **31**, 1940 (1988).
[7]A. J. Brizard, J. Plasma Phys. **41**, 541 (1989).
[8]A. J. Brizard and T. S. Hahm, Rev. Mod. Phys. **79**, 421 (2007).
[9]W. W. Lee, Phys. Fluids **26**, 556 (1983).
[10]S. E. Parker and W. W. Lee, Phys. Fluids B **5**, 77 (1993).
[11]M. Kotschenreuther, G. Rewoldt, and W. M. Tang, Comput. Phys. Commun. **88**, 128 (1995).
[12]Z. Lin, T. S. Hahm, W. W. Lee, W. M. Tang, and R. B. White, Science **281**, 1835 (1998).

[13]F. Jenko, W. Dorland, M. Kotschenreuther, and B. N. Rogers, Phys. Plasmas **7**, 1904 (2000).
[14]J. Candy and R. E. Waltz, J. Comput. Phys. **186**, 545 (2003).
[15]X. Q. Xu, Z. Xiong, M. R. Dorr, J. A. Hittinger, K. Bodi, J. Candy, B. Cohen, R. Cohen, P. Colella, G. Kerbel, S. Krasheninnikov, W. Nevins, H. Qin, T. D. Rognlien, P. B. Snyder, and M. V. Umansky, Nucl. Fusion **47**, 809 (2007).
[16]X. Garbet, Y. Idomura, L. Villard, and T. H. Watanabe, Nucl. Fusion **50**, 043002 (2010).
[17]L. Villard, S. Allfrey, A. Bottino, M. Brunetti, G. Falchetto, V. Grandgirard, R. Hatzky, J. Nührenberg, A. Peeters, O. Sauter *et al.*, Nucl. Fusion **44**, 172 (2004).
[18]S. Wang, Phys. Rev. E **64**, 056404 (2001).
[19]S. Wang, Phys. Plasmas **19**, 062504 (2012).
[20]S. Wang, Phys. Rev. E **87**, 063103 (2013).
[21]S. Wang, Phys. Plasmas **20**, 082312 (2013).
[22]Y. Xu, X. Xiao, and S. Wang, Phys. Plasmas **18**, 042505 (2011).
[23]Y. Xu and S. Wang, Phys. Plasmas **20**, 012515 (2013).
[24]Y. Xu, Z. Dai, and S. Wang, Phys. Plasmas **21**, 042505 (2014).
[25]R. G. Littlejohn, J. Math. Phys. **20**, 2445 (1979).
[26]R. G. Littlejohn, J. Math. Phys. **23**, 742 (1982).
[27]J. R. Cary, Phys. Rep. **79**, 129 (1981).
[28]J. R. Cary and R. G. Littlejohn, Ann. Phys. **151**, 1 (1983).
[29]Z. Dai, Y. Xu, L. Ye, X. Xiao, and S. Wang, Phys. Plasmas **22**, 022301 (2015).
[30]R. J. Goldston, R. B. White, and A. H. Boozer, Phys. Rev. Lett. **47**, 647 (1981).
[31]K. Tani, T. Takizuka, M. Azumi, and H. Kishimoto, Nucl. Fusion **23**, 657 (1983).
[32]R. B. White and H. E. Mynick, Phys. Fluids B **1**, 980 (1989).
[33]M. H. Redi, M. C. Zarnstorff, R. B. White, R. V. Budny, A. C. Janos, D. K. Owens, J. F. Schivell, S. D. Scott, and S. J. Zweben, Nucl. Fusion **35**, 1191 (1995).
[34]M. H. Redi, R. V. Budny, D. S. Darrow, H. H. Duong, R. K. Fisher, A. C. Janos, J. M. McChesney, D. C. McCune, S. S. Medley, M. P. Petrov, J. F. Schivell, S. D. Scott, R. B. White, M. C. Zarnstorff, and S. J. Zweben, Nucl. Fusion **35**, 1509 (1995).
[35]R. Boivin, S. Zweben, and R. White, Nucl. fusion **33**, 449 (1993).
[36]R. G. Littlejohn, Phys. Fluids **24**, 1730 (1981).
[37]R. G. Littlejohn, J. Plasma Phys. **29**, 111 (1983).
[38]J. R. Cary and A. J. Brizard, Rev. Mod. Phys. **81**, 693 (2009).
[39]A. J. Brizard, Phys. Plasmas **2**, 459 (1995).
[40]T. G. Northrop, Rev. Geophys. **1**, 283, doi:10.1029/RG001i003p00283 (1963).
[41]S. Wang, Phys. Plasmas **6**, 1393 (1999).
[42]Y. Idomura, S. Tokuda, and Y. Kishimoto, Nucl. Fusion **43**, 234 (2003).
[43]S. Wang, Phys. Plasmas **13**, 052506 (2006).
[44]Y. Xu and S. Wang, Plasma Phys. Controlled Fusion **55**, 015009 (2013).
[45]X. Xiao and S. Wang, Phys. Plasmas **15**, 122511 (2008).